

# 2

## UTILIZATION OF POLYMER VISCOELASTIC PROPERTIES IN ACOUSTIC WAVE SENSOR APPLICATIONS

SAND--89-0126C

Received by OSTI

S. J. Martin, A. J. Ricco, and G. C. Frye

DE90 010534

Sandia National Laboratories, Albuquerque, NM 87185

MAY 09 1990

### Abstract

The changes which occur in polymer viscoelastic properties in response to cross-linking reactions and due to absorption of gas phase species have been used advantageously in several acoustic wave-based sensor applications. When a polymer film is present on the surface of an acoustic wave device, changes in the viscoelastic properties of the film induce changes in wave propagation velocity and attenuation, providing two sensor responses. Film changes which occur during polymer cross-linking allow photo-polymerization to be monitored in real time using acoustic devices. A photoaction spectrum of photoresist reveals the cross-linking wavelength with maximum quantum yield. Changes in the viscoelastic properties of a polysiloxane film induced by vapor absorption are found to be unique for each of several species, enabling differentiation of species with a single film. A Maxwell model for polymer viscoelasticity, in combination with mass loading effects, provides a sound theoretical basis for explaining observed results for both polysiloxane and polybutadiene/polystyrene copolymer films.

### Introduction

Surface acoustic wave (SAW) and acoustic plate mode (APM) devices have demonstrated utility in a number of gas and liquid phase sensing applications (1-3) as well as in the characterization of thin films (4-7). Propagating acoustic modes are excited and detected by interdigital input and output transducers separated by an interaction region in which the acoustic mode has significant displacement at the device surface. If the acoustic wave medium is coated with a film, propagation of an acoustic wave along the surface results in sinusoidal deformation of the film. Consequently, wave propagation is sensitive to the viscoelastic properties of an overlay. In general, perturbations which change the stored energy density of the wave result in velocity changes, while perturbations which alter power dissipation by the wave result in attenuation changes (8).

In this paper, we investigate acoustic wave responses arising from changing viscoelastic properties of polymer film overlays induced by (1) a photo-cross-linking reaction, and (2) vapor absorption. Various acoustic modes can be used to probe the properties of a film overlay. In the photo-cross-linking reaction, a shear-horizontal (SH) acoustic plate mode (APM) was used (3). The SH-APM, which is excited and detected in a thinned quartz plate, has displacement in the plane of the surface and normal to the direction of mode propagation. In the vapor absorption experiment, a surface acoustic wave (SAW) was used. The SAW has two components of displacement: a shear component normal to the device surface and a compressional component lying in the direction of SAW propagation.

### Monitoring Photo-Cross-Linking Reactions

Cross-linking significantly alters polymer viscoelastic properties. The free movement of one polymer chain relative to its neighbors, which is possible in the uncross-linked polymer, is severely inhibited by the formation of cross-links between chains

(9). The shear modulus of the film in particular provides an indication of the state of cross-linking.

To monitor a photo-cross-linking reaction, negative photoresist films (Waycoat HR-100) were spin-cast at 3000 rpm for 30 seconds directly onto the metallized side of APM devices (over both the IDTs and the wave path), giving a nominal thickness of 1.1  $\mu\text{m}$ . Films were heated to 85 C in air for 10 minutes to remove solvent. HR-100 photoresist consists of partially cyclized polyisoprene, along with 4% (by weight) of a coupling photoinitiator. Absorption of the appropriate wavelength of light by a photoinitiator results in the formation of a cross-link between two polymer chains. To cross-link the resist films, the coated APM device was exposed to monochromatic light produced by a 150 W Xenon lamp coupled to a CVI Laser Digikrom 240 single-pass monochromator. Illumination intensity was approximately 1.2 mW/cm<sup>2</sup> at 370 nm. This wavelength is near the peak spectral sensitivity reported (14) and measured (*vide infra*) for photo-polymerization of HR-100.

Shown in Fig. 1 are the changes in APM propagation velocity  $v$  and attenuation  $\alpha$  measured as the HR-100 film was cross-linked by UV illumination. During the reaction, APM velocity increased while attenuation decreased. After an exposure time of 140 minutes, velocity and attenuation reached stable values, indicating the completion of the cross-linking reaction. The optical energy density incident on the film over this time period was approximately 10.2 J/cm<sup>2</sup>.

Each cross-link formed in the HR-100 film has two effects which give rise to an acoustic wave response: (1) a change in viscoelastic properties due to the formation of a cross-link between polymer chains, and (2) a decrease in surface mass density due to the liberation of two N<sub>2</sub> molecules in the cross-linking reaction (10). As discussed in more detail below, changes in mass density lead to changes in wave velocity, while changes in viscoelastic properties generally cause both wave velocity and attenuation changes.

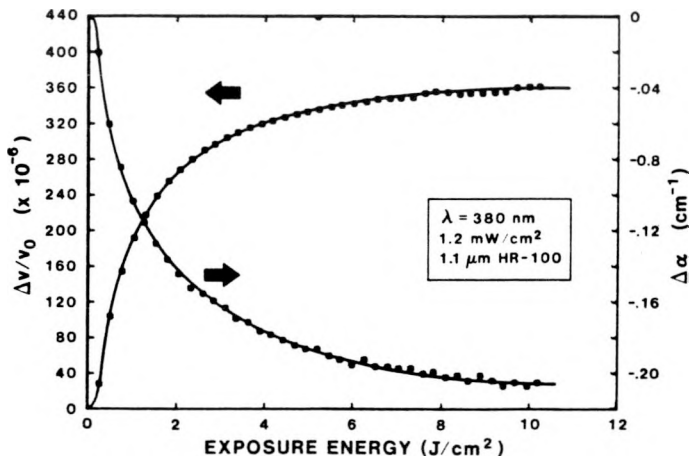


Fig. 1. Changes in APM velocity and attenuation as a function of time measured during cross-linking of HR-100 negative photoresist film.

MASTER

2

## **DISCLAIMER**

**This report was prepared as an account of work sponsored by an agency of the United States Government. Neither the United States Government nor any agency thereof, nor any of their employees, makes any warranty, express or implied, or assumes any legal liability or responsibility for the accuracy, completeness, or usefulness of any information, apparatus, product, or process disclosed, or represents that its use would not infringe privately owned rights. Reference herein to any specific commercial product, process, or service by trade name, trademark, manufacturer, or otherwise does not necessarily constitute or imply its endorsement, recommendation, or favoring by the United States Government or any agency thereof. The views and opinions of authors expressed herein do not necessarily state or reflect those of the United States Government or any agency thereof.**

---

## **DISCLAIMER**

**Portions of this document may be illegible in electronic image products. Images are produced from the best available original document.**

## Spectral Dependence of the Cross-linking Reaction Rate

The wavelength dependence of the photosensitivity of the resist film was determined by measuring the rate at which APM velocity changed in response to cross-linking as a function of incident optical wavelength  $\lambda$ . The time rate of change of APM velocity at each wavelength is defined by:

$$R(\lambda) = \frac{1}{v_0} \frac{dv}{dt}|_{\lambda} \quad (1)$$

Wavelength was stepped under computer control from 200 to 650 nm in 10 nm increments while monitoring the frequency of the resist-coated APM device using the oscillator loop configuration (11). The 15-second dwell time at each wavelength was sufficient for a change in film properties to be measured without appreciably cross-linking the film: the entire spectral response experiment cross-linked the film by less than 20%. In a second wavelength scan, the spectral density  $I(\lambda)$  of the source was determined using a pyroelectric detector. The relative spectral sensitivity for film cross-linking is then  $R(\lambda)/I(\lambda)$ .

The cross-linking rate of the HR-100 photoresist film vs. optical wavelength is shown in Fig. 2 (•). The peak in spectral sensitivity is at approximately 370 nm, in reasonable agreement with the sensitivity peak of 360 nm cited by the manufacturer (10). Also shown in Fig. 2 (x) is a UV-visible absorbance spectrum recorded for an identically prepared 1.1  $\mu\text{m}$ -thick HR-100 film spin-coated onto a quartz substrate. Absorbance was measured over the 200 to 650 nm range using a Varian/Cary 2300 spectrophotometer. The absorbance spectrum has a peak at 355 nm, corresponding to the peak observed in the acoustic measurement of  $R(\lambda)/I(\lambda)$ . The film also exhibits very high absorbance at wavelengths below 300 nm, a result *not* observed in the acoustic measurement.

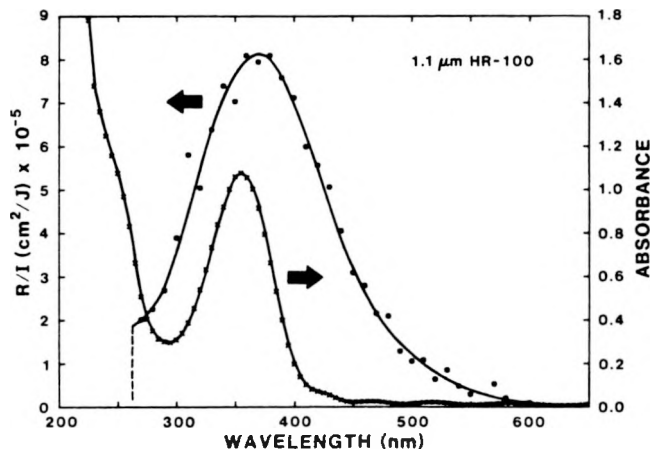


Fig. 2. Acoustically probed photoaction spectrum of HR-100 photoresist film (left axis); rate of change of APM velocity  $R(\lambda)$ , normalized to spectral density  $I(\lambda)$ , indicates rate of film cross-linking as a function of wavelength  $\lambda$ . Optical absorption spectrum of identical film (right axis).

The spectral response measured using the acoustic wave device is an *action* spectrum in that only optical absorptions which lead to a chemical reaction and thereby contribute to changes in the elasticity or density of the film are registered. The peak in the absorbance spectrum (Fig. 4, x) at 355 nm is due to photoinitiator absorption, which leads to the formation of cross-links in the polymer and a corresponding peak in the acoustic  $R(\lambda)/I(\lambda)$  response at 370 nm. The strong absorption at wavelengths less than 300 nm, however, is likely due to the polymer backbone

(cyclized polyisoprene), which is not photoactive; thus, its optical absorption affects neither mass density nor the elastic properties of the film.

## Viscoelastic Changes Induced by Vapor Absorption

The absorption of gas-phase species by a polymer film has several effects on SAW propagation. A decrease in SAW velocity due to the increased mass density has been well documented (1). In addition, small molecules which are molecularly dispersed in a polymer tend to plasticize the polymer, thereby changing the viscoelastic properties (9). In general, the relative contributions to velocity and attenuation changes made by different species are unique, enabling species to be discriminated on this basis.

Perturbations in SAW velocity and attenuation were measured with a polysiloxane-coated SAW device during exposure to organic vapors over a wide range of concentrations. The 1.0  $\mu\text{m}$ -thick polysiloxane film was deposited by plasma-assisted chemical vapor deposition, using hexamethyldisiloxane, onto the surface of a 97 MHz SAW device. Shown in Fig. 3 is the manner in which velocity and attenuation vary in the polysiloxane-coated device as vapor concentration varies. Each data set is a parametric representation of an absorption isotherm--the locus of  $(\Delta v/v_0, \Delta \alpha/k)$  points measured as solvent partial pressure varied from 0 to 97% of saturation (in nitrogen at 20 °C) and back again. (For some species, the propagation loss became so large that the maximum concentration was set by the point at which insertion loss reached 65 dB.) The responses recorded during absorption and desorption track well over the two hour concentration ramp. Each vapor generates a unique locus of  $(\Delta v/v_0, \Delta \alpha/k)$  points, enabling chemical differentiation on the basis of this two-parameter response. Conventional SAW gas/vapor sensors rely on velocity perturbations alone (12), necessitating the use of multiple films for discrimination.

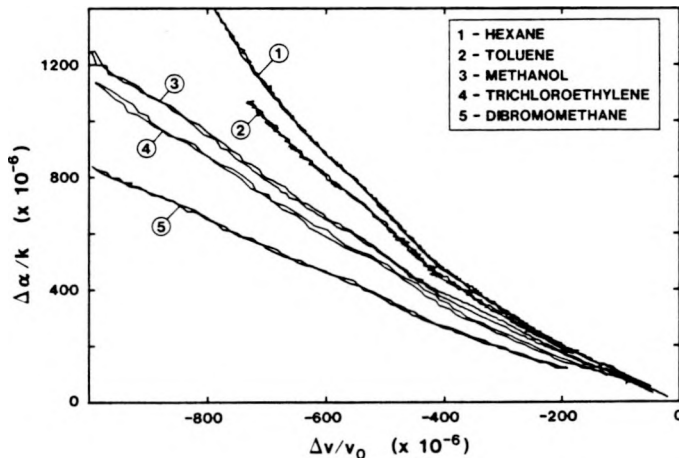


Fig. 3. Attenuation per wavenumber vs. fractional velocity shift due to solvent vapor absorption by a polysiloxane-coated SAW device. Each vapor generates a unique locus of  $(\Delta v/v_0, \Delta \alpha/k)$  points, enabling differentiation of species on the basis of these two responses.

Velocity and attenuation changes measured during vapor sorption are due, to a large extent, to viscoelastic changes occurring in the film. The perturbation in SAW propagation caused by a thin-film viscoelastic overlay may be determined from a perturbation calculation. For several of the polymer films examined, the viscoelastic behavior can best be described by a simple Maxwell model, shown in Fig. 4. In this model, the viscous element (shear viscosity  $\eta$ ) represents the frictional resistance of polymer chains to flowing past one another (9). The elastic element (shear stiffness

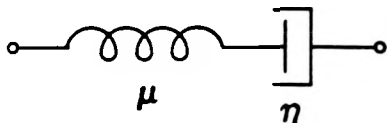


Fig. 4. The simple Maxwell model which best describes the shear viscoelastic behavior of the polymer films examined. Solvent absorption causes plasticization (reducing effective viscosity  $\eta$ ) so that polymer changes from elastic to viscous behavior.

$\mu$ ) represents restoring forces arising from the tendency of polymer chains to seek their most probable configuration. The ratio of shear stress to shear strain in the polymer is given by the complex shear modulus  $G = G' + jG''$ . The real part,  $G'$ , is the storage modulus, while  $G''$  is the loss modulus. A shear relaxation time  $\tau = \eta/\mu$  gives the time scale for sinusoidal deformation (with angular frequency  $\omega$ ) at which the material changes from elastic to viscous behavior: for  $\omega\tau >> 1$ , the material behaves elastically with  $G = \mu$  (thus  $\mu$  represents the glassy shear modulus of a polymer); for  $\omega\tau << 1$  the material behaves viscously with  $G = j\omega\eta$ .

The changes in SAW velocity and attenuation due to a Maxwellian viscoelastic film are given by:

$$\frac{\Delta v}{v_0} = -\omega h \left[ c_1 \rho + c_2 \frac{\mu(\omega\tau)^2}{1 + (\omega\tau)^2} \right] \quad (2a)$$

$$\frac{\Delta \alpha}{k} = c_2 \omega h \left( \frac{\mu \omega \tau}{1 + (\omega\tau)^2} \right), \quad (2b)$$

where  $\omega$  and  $k$  are the angular SAW frequency and wavenumber, respectively;  $\rho$ ,  $h$  and  $\tau$  are the mass density, thickness and shear relaxation time, respectively, of the film;  $c_1$  and  $c_2$  are substrate-dependent constants (13). This result holds under the following assumptions: (1) film thickness is small compared with the acoustic wavelength, and (2) the magnitude of the film's bulk modulus is large compared with the shear modulus. The latter assumption is typically valid for polymers (14). The term involving  $c_1$  in Eqs. 2 describes the effect of film mass density on SAW propagation; terms involving  $c_2$  constitute the viscoelastic response. In general, changes in mass density affect only wave velocity, while viscoelastic changes affect both velocity and attenuation.

The viscoelastic velocity and attenuation changes given in Eqs. 2 take the form of a relaxation response. If the film is initially in the elastic (glassy) state (with  $\omega\tau >> 1$ ) and goes through a transition to the viscous state ( $\omega\tau << 1$ ), the SAW velocity increases monotonically, while attenuation goes through a peak at  $\omega\tau = 1$ . This behavior, which can be elicited by heating the film (15), is analogous to the zero-frequency glass transition.

An elastic-to-viscous transition can also be exhibited by a polymer film upon absorption of gas phase species. Small molecules which are molecularly dispersed in a polymer tend to plasticize the polymer, lowering the local friction between polymer chains and decreasing the effective viscosity  $\eta$  (9). (We are neglecting here any chemical interactions between polymer and solvent, such as hydrogen bonding, which may also contribute to elastic changes.) In comparison to the large changes in viscosity which accompany this plasticization,  $\mu$  is relatively unchanged, so that  $\tau$  varies directly with  $\eta$ . The decrement in viscosity and relaxation time due to solvation of gas phase species is a physical effect found to vary exponentially with the volume fraction of the solvent present (9). Up to solvent volume fractions of approximately 30%, this may be expressed as:

*measured volume?*

$$\tau = \tau_0 \exp\left(\frac{-\gamma NV}{1 + NV}\right) \quad (3)$$

where  $\tau_0$  is the relaxation time of the pure polymer,  $N$  is the number of solvent molecules per volume of pure polymer,  $V$  is the species volume, and  $\gamma$  is a constant.

In order to observe the entire range of viscoelastic behavior predicted by Eqs. 2, SAW operating frequency and film properties must be such that  $\omega\tau$  can be varied widely with respect to unity. With a SAW device having a center frequency of 97 MHz, a film whose relaxation time can easily be varied over this range is a copolymer of polybutadiene and polystyrene (PBPS). A 0.34  $\mu\text{m}$ -thick PBPS film (composition: 80% polybutadiene, 20% polystyrene) was spin-cast onto a 97 MHz ST-cut quartz SAW device. (Very similar behavior to that reported below was observed with uncross-linked poly-1,2-butadiene, but without attaining as large a range in  $\omega\tau$ .)

In addition to causing plasticization, vapor absorption leads to an increase in surface mass density:

$$\Delta(\rho h) = N m h \quad (4)$$

where  $m$  is the mass of each vapor molecule absorbed.

The manner in which SAW velocity and attenuation vary during absorption and desorption of trichloroethylene by the PBPS film is shown in Fig. 5. The responses recorded during absorption and desorption track well over the two hour concentration ramp. When velocity and attenuation changes recorded during the isothermal measurement are plotted against each other, the data display a distinctive loop in the  $\Delta v/v_0$ - $\Delta\alpha/k$  plane. The shape of the isotherm is determined by the relative rates at which plasticization and mass loading occur during vapor absorption. The plasticizing action of absorbed species results in a semi-circle in the first quadrant of the  $\Delta v/v_0$ - $\Delta\alpha/k$  plane (15), while the mass contribution pulls these points toward lower velocity. Thus, the isothermal loop arises from a superposition of mass-loading and plasticization by the absorbed species.

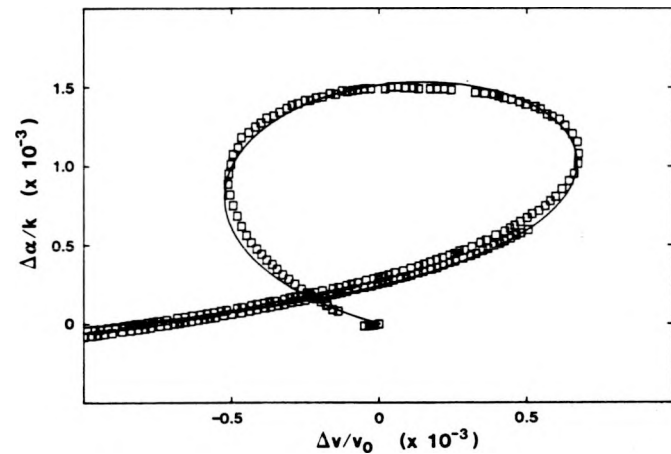


Fig. 5. Attenuation per wavenumber vs. velocity change due to absorption of trichloroethylene by a polybutadiene/polystyrene copolymer-coated SAW device. The data display an elastic-to-viscous relaxation caused by plasticization of the film by the vapor. The solid line, calculated from Eqs. 2 - 4, is based on a superposition of mass-loading and plasticization by the absorbed species.

The solid line in Fig. 3 shows how calculated values of  $\Delta v/v_0$  and  $\Delta\alpha/k$ , based on Eqs. 2 - 4, vary with solvent concentration  $N$ .

In this calculation, N was varied from 0 to  $4 \times 10^{20}$  /cm<sup>3</sup>, with attenuation reaching a maximum for a volume fraction of approximately 20%. Best-fit model parameters were chosen as:  $\mu = 6.9 \times 10^{10}$  dyne/cm<sup>2</sup>,  $\omega_r = 15$ ,  $\gamma = 0.013$ . The calculated variation in  $\Delta v/v_0$  and  $\Delta a/k$  follows experimentally measured values quite well. While the ability to fit the data with three parameters is not surprising, the same model parameters will also predict a diversity of data taken during absorption of pentane, methylene chloride, dibromomethane, as well as during a temperature ramp (15).

## Conclusions

Acoustic wave devices function effectively as real-time monitors of cross-linking reactions. The relative spectral sensitivity of a photoreaction can be determined from the rate of change of APM velocity as a function of optical wavelength.

Perturbations in SAW velocity and attenuation observed in some uncross-linked polymer films can be explained with a perturbational calculation based on a Maxwellian constitutive relationship for the film. This model accounts for responses observed during elastic-to-viscous transitions accompanying vapor absorption by films. The total response is a superposition of a viscoelastic response, arising from polymer plasticization, together with a mass-loading contribution.

With regard to gas/vapor sensing applications, SAW viscoelastic responses are significant when Maxwellian film properties are such that  $\omega_r$  is within an order of magnitude of unity. Since each vapor generates a unique locus of ( $\Delta v/v_0$ ,  $\Delta a/k$ ) points, species can be discriminated by simultaneous measurement of these parameters during the vapor plasticization process (16). For  $\omega_r >> 1$  or  $\omega_r << 1$ , the incremental changes in velocity should be dominated by mass changes. In this regime, velocity will decrease with solvent concentration without significant changes in attenuation.

## Acknowledgements

The authors are indebted to B. J. Lammie of Sandia National Laboratories for expert technical assistance. Valuable technical discussions with D. B. Adolf, K. S. Schweizer, L. R. Gilliom, and T. Tanaka are also acknowledged. This work was performed at Sandia National Laboratories and supported by the U.S. Department of Energy under contract No. DE-AC0476DP00789.

## References

1. H. Wohltjen and R. Dessim, "Surface Acoustic Wave Probe for Chemical Analysis", *Anal. Chem.*, **51** (1979) 1458-1475.
2. R. Lee, J. F. Vetelino, R. S. Falconer, and Z. Xu, "Prototype Microwave Acoustic Fluid Sensors", *Proc. 1988 IEEE Ultrasonics Symp.*, pp. 585-589.
3. S. J. Martin, A. J. Ricco, T. M. Niemczyk, and G. C. Frye, "Characterization of SH Acoustic Plate Mode Liquid Sensors", *Sensors and Actuators*, **20** (1989) 253-268.
4. D. S. Ballantine, Jr. and H. Wohltjen, "Use of SAW Devices to Monitor Visco-elastic Properties of Materials", *Proc. 1988 IEEE Ultrasonics Symp.*, pp. 559-562.
5. E. T. Zellers, R. M. White, and S. W. Wenzel, "Computer Modelling of Polymer-Coated ZnO/Si Surface-Acoustic-Wave and Lamb-Wave Chemical Sensors", *Sensors and Actuators*, **14** (1988) 35-45.
6. J. A. Groetsch III and R. E. Dessey, "A Surface Acoustic Wave (SAW) Probe for the Thermomechanical Characterization of Selected Polymers", *J. Appl. Polymer Science*, **28** (1983) 161-178.
7. G. C. Frye, S. J. Martin, and A. J. Ricco, "Monitoring Diffusion in Real Time in Thin Polymer Films Using SAW Devices", *Sensors and Materials*, **1** (1989) 335-357.
8. S. J. Martin and A. J. Ricco, "Effective Utilization of Acoustic Wave Sensor Responses: Simultaneous Measurement of Velocity and Attenuation", *Proc. 1989 IEEE Ultrasonics Symp.*, 621-625.
9. J. D. Ferry, *Viscoelastic Properties of Polymers*, Third Ed., Wiley, New York, 1980.
10. A. Stein, "The Chemistry and Technology of Negative Photoresists", Olin-Hunt Chemical Co., Palisades Park, N.J.
11. S. J. Martin and A. J. Ricco, "Monitoring Photo-polymerization of Thin Films Using SH Acoustic Plate Mode Sensors", *Sensors and Actuators*, Vol. A, No. 22 (1990) 712-718.
12. M. S. Nieuwenhuizen and A. Venema, "Surface Acoustic Wave Chemical Sensors", *Sensors and Materials*, **5** (1989) 261-300.
13. For SAWs propagating along the X-crystalline direction of ST-quartz:  $c_1 = 2.03 \times 10^7$  cm<sup>2</sup>/s/g,  $c_2 = 2.47 \times 10^{11}$  s<sup>3</sup>/g.
14. D. S. Ballantine, Jr. and H. Wohltjen, "Elastic Properties of Thin Polymer Films Investigated with Surface Acoustic Wave Devices", *Chemical Sensors and Microinstrumentation* (ACS, Washington, 1989) Ch. 15.
15. S. J. Martin and G. C. Frye, "SAW Response to Changes in Viscoelastic Film Properties", in preparation for *Appl. Phys. Lett.*
16. G. C. Frye and S. J. Martin, "Dual Output Acoustic Wave Sensors for Molecular Identification", in preparation for *Anal. Chem.*

## DISCLAIMER

This report was prepared as an account of work sponsored by an agency of the United States Government. Neither the United States Government nor any agency thereof, nor any of their employees, makes any warranty, express or implied, or assumes any legal liability or responsibility for the accuracy, completeness, or usefulness of any information, apparatus, product, or process disclosed, or represents that its use would not infringe privately owned rights. Reference herein to any specific commercial product, process, or service by trade name, trademark, manufacturer, or otherwise does not necessarily constitute or imply its endorsement, recommendation, or favoring by the United States Government or any agency thereof. The views and opinions of authors expressed herein do not necessarily state or reflect those of the United States Government or any agency thereof.